Cell Tissue Res (1991) 265:317–328

Cell and Tissue Research



# An electron-microscope and freeze-fracture study of the egg cortex of *Brachydanio rerio*

**Nathan H. Hart**[1] **and Gregory C. Collins**[2]

[1] Department of Biological Sciences, Nelson Biology Laboratories-Bush Campus, P.O. Box 1059, Piscataway, NJ 08855-1059, USA
[2] Department of Biological Sciences, Rutgers University, New Brunswick, NJ 08903, USA

Accepted March 1, 1991

**Summary.** We have examined the cortex of the teleost (*Brachydanio rerio*) egg before and during exocytosis of cortical granules by scanning, transmission, and freeze-fracture electron microscopy. In the unactivated egg, the P-face of the plasma membrane exhibits a random distribution of intramembranous particles, showing a density of 959/$\mu m^2$ and an average diameter of 8 nm. Particles over P- and E-faces of the membranes of cortical granules are substantially larger and display a significantly lower density. An anastomosing cortical endoplasmic reticulum forms close associations with both the plasma membrane of the egg and the membranes of cortical granules. Exocytosis begins with cortical granules pushing up beneath the plasma membrane to form dome-shaped swellings, coupled with an apparent clearing of particles from the site of contact between the apposed membranes. A depression in the particle-free plasma membrane appears to mark sites of fusion and pore formation between cortical granules and plasma membranes. Profiles of exocytotic vesicles undergo a predictable sequence of morphological change, but maintain their identity in the egg surface during this transformation. Coated vesicles form at sites of cortical granule breakdown. Differences in particle density between cortical granules and egg plasma membranes persist during transformation of the exocytotic profiles. This suggests that constituents of the 2 membrane domains remain segregated and do not intermix rapidly, lending support to the view that the process of membrane retrieval is selective (i.e., cortical granule membrane is removed).

**Key words:** Cortical reaction, ovum – Exocytosis – Cell membrane – Cortical granules, ovum – Intramembranous particles – *Brachydanio rerio* (Teleostei)

The cortex of the animal egg is the site of massive and global reorganization at fertilization. Within minutes of sperm-egg union, membrane-limited cortical granules fuse with the plasma membrane of the egg, rupture, and discharge their contents into the extracellular space (Eddy and Shapiro 1976; Chandler and Heuser 1979; Hart and Yu 1980; Longo 1981, 1988). Exocytosis follows a transient increase in cytoplasmic $Ca^{+2}$ released from intracellular storage sites (Gilkey et al. 1978; Yoshimoto et al. 1986; Iwamatsu et al. 1988). Subsequently, membrane is removed from the egg surface by endocytosis and transported into the cortical cytoplasm (Fisher and Rebhun 1983; Carron and Longo 1984; Donovan and Hart 1986). The released contents of the cortical granules contribute to the formation of extracellular envelopes which block polyspermy and protect the embryo from environmental insult (Kay and Shapiro 1985).

Our knowledge of egg structure and of the breakdown of cortical granules is based principally on sea urchin eggs (Longo 1988). Cortical granules in unfertilized sea urchin eggs appear to be tightly bound to the cytoplasmic face of the plasma membrane, a connection sufficiently strong to survive forces encountered during the isolation of exocytotically-competent fractions of membranes from the egg cortex (Detering et al. 1977; Vater and Jackson 1989). The plasma membrane is dome-shaped and lacks intramembranous particles (IMPs) over those regions occupied by the cortical granules (Longo 1981; Zimmerberg et al. 1985). This suggests that predetermined fusion-sites are in place on the plasma membrane before exocytosis of cortical granules is initiated. In other studies, however, a random and uniform distribution of IMPs over plasma membranes of sea urchin eggs (Chandler and Heuser 1979) has been reported.

Fusion between the plasma membrane and membranes of the cortical granules produces a new mosaic surface that consists of 2 domains: the original plasmalemma of the egg and the membranes formerly delimiting the cortical granules (Hart et al. 1977; Longo 1981; Carron and Longo 1984; Donovan and Hart 1986). Although the 2 domains are morphologically distinct (Hart and Yu 1980; Longo 1981), questions remain concerning

*Offprint requests to:* N.H. Hart

their fate and integration into the activated egg surface. Several studies have indicated that the mosaic character of the egg surface is temporary with discernible differences between the 2 membrane domains quickly lost (Longo 1981; Carron and Longo 1984). Differences in IMP density between fractured membranes of cortical granules and the plasma membranes, for example, are not apparent in the activated egg surface of *Arbacia* (Longo 1981). By contrast, patches of cortical granule membrane appear to persist in the mosaic egg surface of *Strongylocentrotus* and do not mix with the egg plasma membrane (Chandler and Heuser 1979). This suggests that there may be constraints on lateral diffusion of components of cortical granule membranes in the fluid bilayer of the egg surface.

It is now well-established that exocytosis is followed by the removal of surface membrane in the form of coated vesicles (Donovan and Hart 1982, 1986; Fisher and Rebhun 1983; Carron and Longo 1984). The composition and source of the internalized membrane are uncertain. Although coated vesicles in echinoderm eggs appear to form at sites of the mosaic surface presumably originating from cortical granules (Fisher and Rebhun 1983), the rapid intermixing of molecular and structural components of the fused membranes eliminates any distinction between specific membrane segments (Longo 1981; Carron and Longo 1984). Profiles of exocytosis in activated eggs of the zebrafish (*Brachydanio*) and the chum salmon (*Oncorhynchus*) are temporally and morphologically associated with coated pits and forming coated vesicles (Kobayashi 1985; Donovan and Hart 1986). Such observations strongly suggest that membrane is retrieved selectively from the domains of cortical granule membranes, but further investigation of the properties of the mosaic surface would be useful to answer this question.

In this study, we have employed the large, translucent egg of the zebrafish (*Brachydanio*) and techniques of scanning, transmission, and freeze-fracture electron-microscopy to study the egg cortex before and after activation, with particular focus on the cortical granules and their relationship to the plasma membrane. The density and size of IMPs were used to describe the organization of cortical granule membranes and egg plasma membrane prior to and during exocytosis. Our observations reveal that: (1) differences in IMP density (P-face) between plasma membrane and cortical granule membranes persist in the activated egg surface during reorganization of exocytotic profiles; and (2) coated vesicles originate on the mosaic egg surface from domains derived from cortical granule membranes.

## Materials and methods

### *Eggs*

Eggs were obtained from adult, gravid females of *Brachydanio* using previously reported techniques (Hart and Messina 1972). Cells were then either fixed immediately (unactivated) or immersed in filtered, dechlorinated tap water for activation. *Brachydanio* eggs have been shown to undergo normal activation under these conditions (Hart and Yu 1980; Donovan and Hart 1986). Eggs were fixed in glutaraldehyde at selected intervals through 4–5 min post-activation.

### *Freeze-fracture*

Unactivated and activated eggs were fixed in 3% glutaraldehyde in 0.1 M phosphate buffer (pH 7.3) containing 4% sucrose for 3 h at room temperature. The chorion was then removed manually from most unactivated eggs and all activated eggs using Dumont No. 5 forceps. All cells were cryoprotected by the gradual addition of glycerol in 0.1 M phosphate buffer to a final concentration of 30%. Eggs were mounted in gold center-well specimen holders and quickly frozen by immersion in melting Freon 22 cooled with liquid nitrogen. Samples were knife-fractured in a Balzers 301 Freeze Etch Unit (Balzers Corp., Hudson, NH) at −120° C, without etching, and replicated with platinum-carbon from an electron-beam gun mounted at 45°. Replicas were backed with carbon applied at 90°, cleaned in full-strength bleach, washed in distilled water, and mounted on 300 mesh copper grids for viewing with a Philips EM 300 microscope operated at 80 kV.

The density of intramembranous particles (IMPs/$\mu m^2$) over fractured membranes of cortical granules and plasma membranes was determined from micrographs of replicas enlarged to a final magnification of approximately 100000 diameters. An acetate overlay divided into grid squares of known size was attached to the micrograph and direct counts of IMPs then made with the aid of a telecentric lupe. Particle counts of the egg plasma membrane excluded squares that contained fractured microplicae. A total of 1.5 and 1.2 $\mu m^2$ of plasma membrane and 3.0 and 1.1 $\mu m^2$ of cortical granule membrane were examined from unactivated and activated eggs, respectively. The counts for each membrane domain were pooled and the significance of differences then calculated using a two-tailed Student *t*-test. IMP size (diameter) was determined using the technique of Goodenough and Staehlin (1971) by measurement of the widest part of the particle shadow with a 7x telecentric lupe equipped with a micrometer grating.

Fracture faces were identified as either "P" (protoplasmic leaflet) or "E" (extracellular leaflet) according to the convention of Branton et al. (1975). The freeze-fracture micrographs are presented in the form that platinum deposits are black and shadows are white.

### *Electron microscopy*

For either scanning (SEM) or transmission (TEM) electron microscopy, eggs were fixed in 2% glutaraldehyde in 0.1 M cacodylate buffer (pH 7.3), containing 4% sucrose, for 2 h at 4° C. Fixed cells for SEM were rinsed in buffer, treated with 1% $OsO_4$ in 0.1 M cacodylate buffer, dehydrated in a graded series of ethanols, and critical-point dried with Freon 13. They were then coated with gold-palladium and examined in an Hitachi S-450 scanning electron microscope operated at either 15 or 20 kV. Cells for TEM were processed according to Donovan and Hart (1986), and ultrathin sections were viewed in a Philips 300 electron microscope operated at 80 kV.

**Fig. 1a–c.** Unactivated egg cortex. **a** SEM micrograph of cross-fractured egg showing plasma membrane (*P*) decorated with reticulum of small folds and cortical granules (*CG*). ×5175. **b** Regionalization of the cortical cytoplasm into outer, electron-dense layer (*small arrowheads*) and deeper, less compact layer with cortical granules (*CG*). *CV* coated vesicles; *M* mitochondria; *L* lysosomes. *Large arrowheads* point to profiles of CER. ×25000. **c** P-face (*P*) and E-face (*E*) surfaces of fractured membranes of cortical granules. *Large arrow* indicates direction of shadowing. ×29450

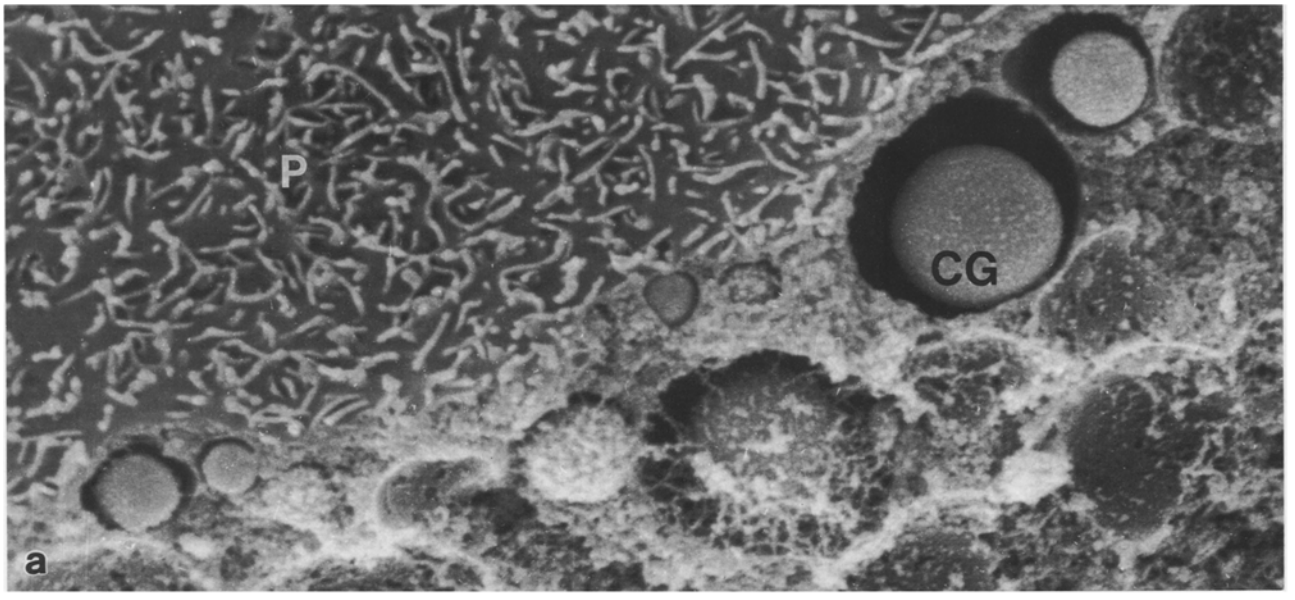
P
CG
a

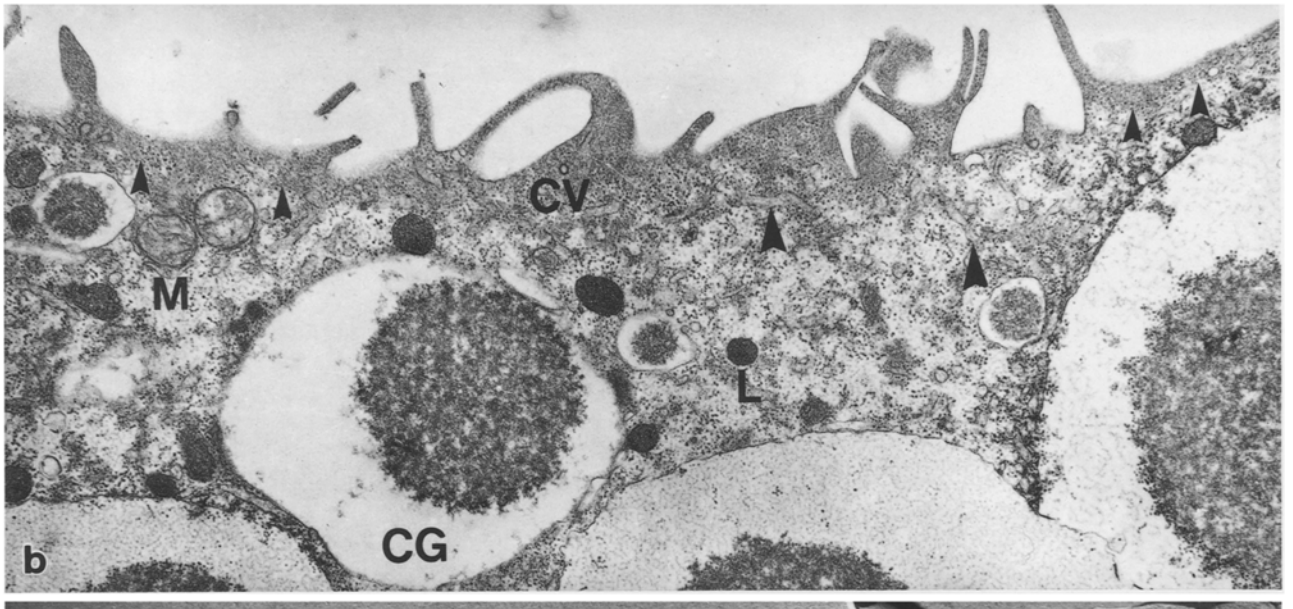
CV
M
L
CG
b

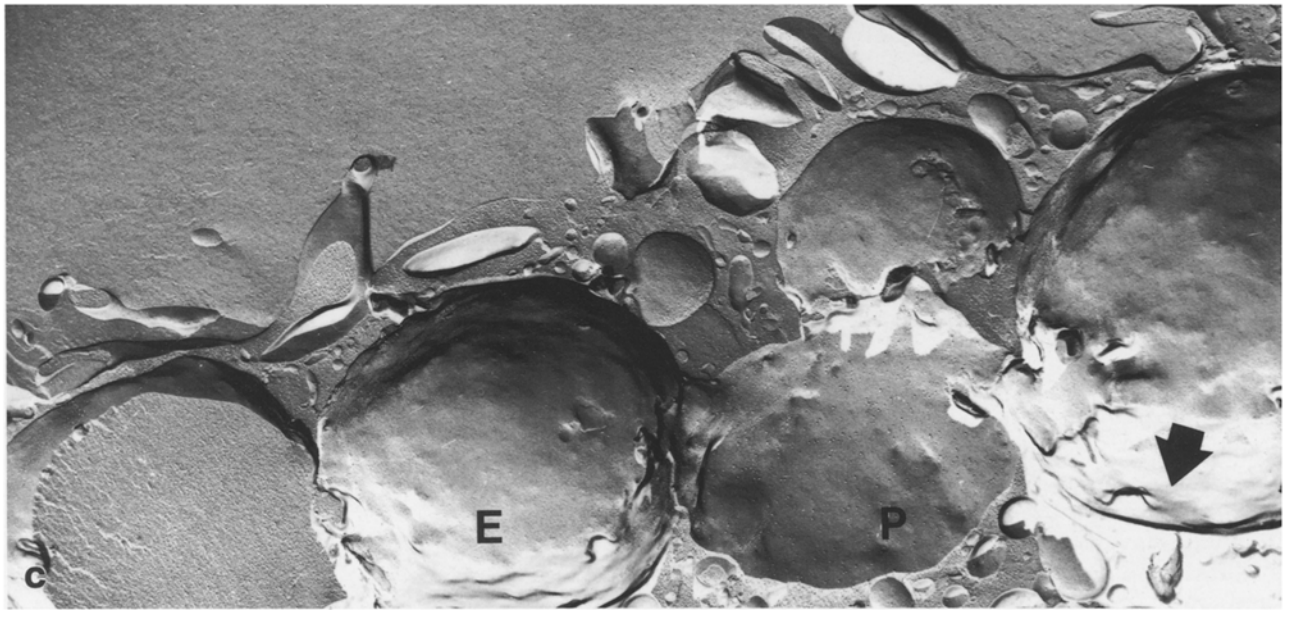
E
P
c

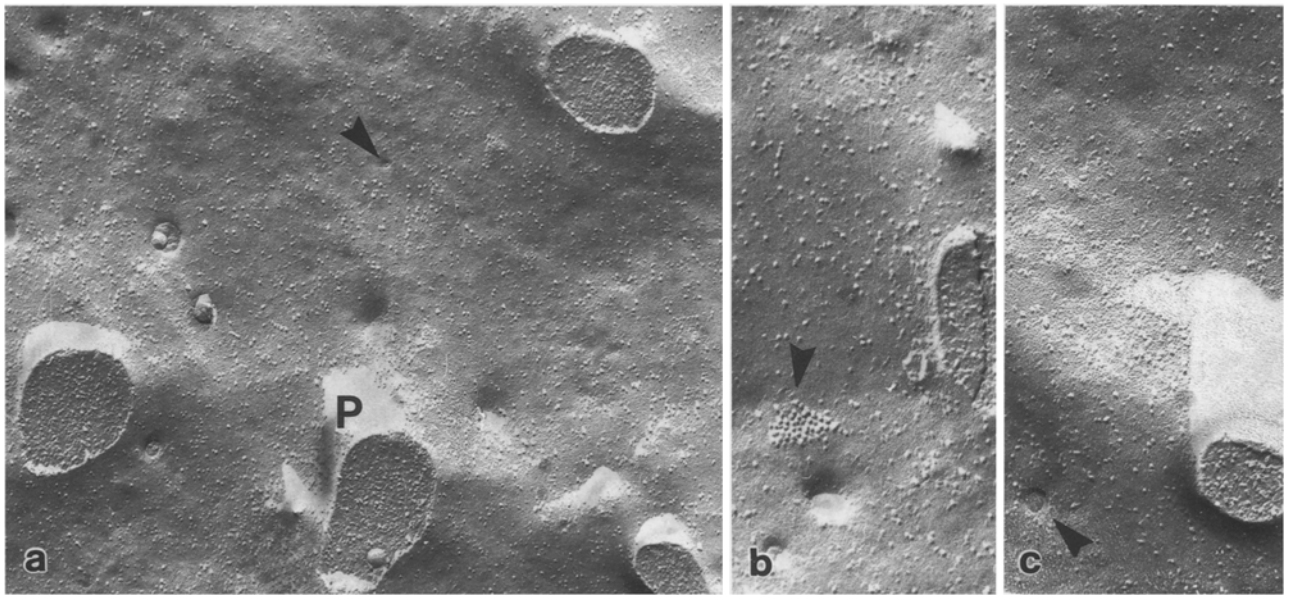


**Fig. 2a–c.** P-face replicas of unactivated egg plasma membrane. **a** Distribution of IMPs between stumps of fractured microplicae (*P*). Note small circular depressions (*arrowhead*) in fracture plane. ×27930. **b** Clusters of particles (*arrowhead*) are occasionally observed over P-face. ×79450. **c** Higher magnification of small circular profile (*arrowhead*) noted in **a**. ×79800

## Results

### *Cortical structures of the unactivated egg*

The cortex of the unactivated zebrafish egg included the plasmalemma and the peripheral cortical cytoplasm with various organelles. The plasmalemma under SEM displayed a reticulum of small folds or microplicae scattered over an otherwise smooth-appearing surface (Fig. 1a). In single planes of section, the microplicae were electron-dense and appeared as finger-shaped projections that measured about 0.9 μm in height and 0.15 μm across the base (Fig. 1b). These folds, in the intact egg, extended into the pore canals of the extracellular chorion. The cortical cytoplasm itself was organized into a narrow, electron-dense zone subjacent to the plasma membrane and a deeper region in which the cytoplasm appeared less compact (Fig. 1b). The electron-dense layer was about 200 nm in width and typically lacked most of the intracellular organelles found in the rest of the cortex, although profiles of the endoplasmic reticulum and an occasional coated vesicle could be detected at this site (Fig. 1b). The most conspicuous organelles of the cortex were the cortical granules, and these were readily recognized by their location, spherical shape, and size in either SEM images, ultrathin sections, or freeze-fracture replicas (Fig. 1a–c). Views of cross-fractured whole eggs, following either critical-point drying or platinum-carbon replication, confirmed observations on ultrathin sections showing that cortical granules were organized as irregular rows and always separated from the plasma membrane by cytoplasm (Fig. 1a–c). Other organelles of the deeper cortical cytoplasm included annulate lamellae, mitochondria, circular and tubular profiles of smooth endoplasmic reticulum, lysosomes, and Golgi apparatus (Figs. 1b, 5a).

### *The plasma membrane*

Microplicae of the plasma membrane typically broke during the fracturing process and left an array of stump-like projections over the P-face (Fig. 2a). IMPs were identified between stumps of the microplicae; their distribution appeared to be relatively homogeneous and random over the P-face (Fig. 2a). Hence, the P-face fracture displayed no specialized arrangement of particles that might represent predetermined sites of fusion between cortical granules and the plasma membrane upon exocytosis. The mean density of IMPs (P-face) was 959±176 particles/μm² (Table 1). The diameters of the

**Table 1.** Particle densities on fracture faces of plasma and cortical granule membranes of zebrafish eggs. Data presented as mean number of intramembranous particles per μm² (X±SD) of membrane and analyzed by 2-tailed Student *t*-test. In replicas of activated eggs, membranes formerly delimiting cortical granules were recognized either by crypt-like or flattened morphology. IMPs counted from flattened profiles. Level of significance, 5%. (A) significantly different from (C), (D) and (E); (B) significantly different from (C), (D) and (E); (C) significantly different from (A), (B) and (E); (D) significantly different from (A), (B), and (E); (E) significantly different from (A), (B), (C) and (D). *N*, Number of sample areas counted for each domain

| | Mean no. particles/μm² | | | |
|---|---|---|---|---|
| | *N* | Unactivated | *N* | Activated |
| Plasmalemma | | | | |
| P-face | 44 | 959±176 (A) | 37 | 672±155 (B) |
| E-face | – | Not observed | – | Not observed |
| Cortical granule membrane | | | | |
| P-face | 35 | 263±81 (C) | 31 | 300±97 (D) |
| E-face | 32 | 39±25 (E) | – | Not observed |

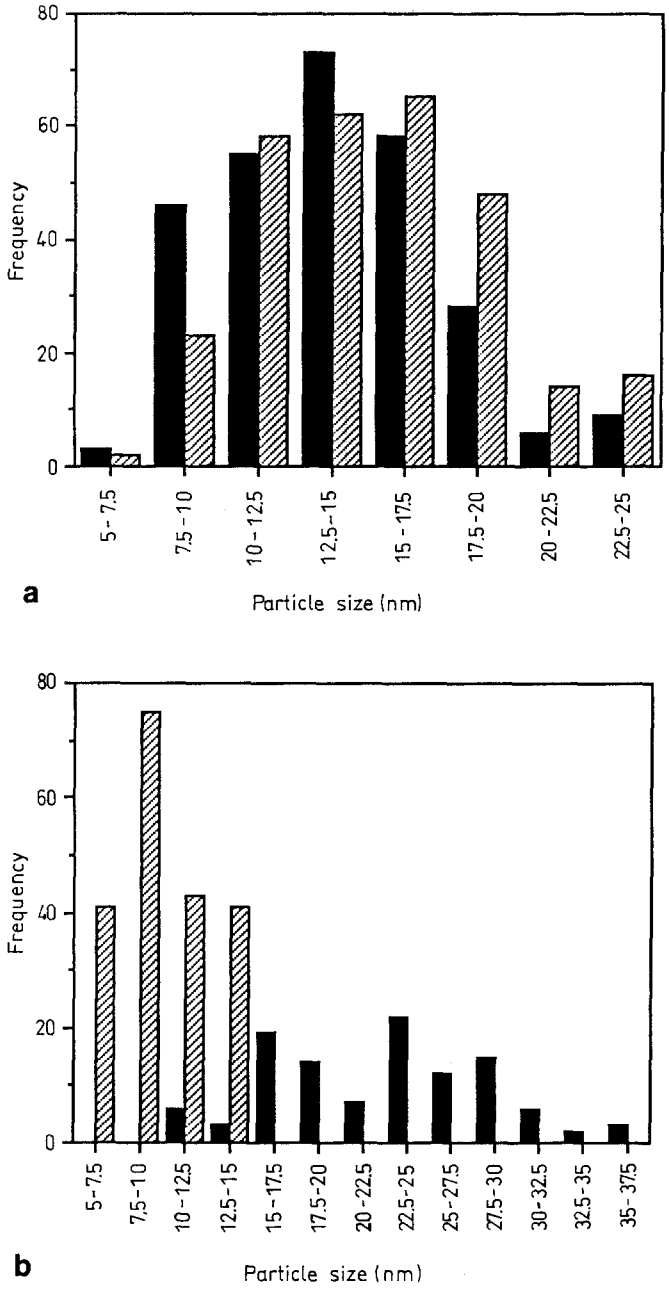


**Fig. 3a, b.** Histograms showing range of particle diameters (*abscissa*) and frequency (*ordinate*) for (**a**) P- (■) and E- (▨) faces of cortical granule membranes of unactivated eggs, and (**b**) P-face of plasma membrane of unactivated (▨) and activated (■) eggs

IMPs over the P-face ranged from 5.0 to 15.0 nm, with the mean diameter recorded as $8.4 \pm 3.3$ nm (Fig. 3; $N = 200$). Occasionally, tightly-packed clusters of IMPs were encountered over the P-face between microplicae (Fig. 2b). These displayed considerable variation in number and configuration of IMPs. We have also observed small, pore-like structures measuring 25–50 nm in diameter scattered over the same fracture-face (Fig. 2a, c). The E-face of the unactivated egg plasma membrane was rarely encountered in our replicas, which precluded any systematic analysis of its IMPs.

*The cortical granules*

The cortical granules of eggs prepared for freeze-fracture appeared to be very fragile. In the same frozen cell, we occasionally observed that fractured membranes of some cortical granules were continuous and intact, while in other granules the limiting membranes had ruptured and allowed leakage of cytoplasm into the organelle. Both P- and E-faces of cortical granule membranes exhibited a population of IMPs (Fig. 4a, b). Similar to the plasma membrane (Figs. 2a, 4c), IMPs over the membranes of cortical granules appeared to be homogeneous and randomly-spaced (Fig. 4a, b). However, as summarized in Table 1, the mean particle density on the P-face was significantly lower ($263 \pm 81$ nm; Fig. 4a) than that of the same fracture-face of the plasma membrane (Fig. 4c), but significantly higher than the IMP density over the E-face of the cortical granule membrane ($39 \pm 25$ nm; Fig. 4b). Furthermore, the diameters of IMPs over the membranes of cortical granules were substantially larger that those over the P-face of the plasma membrane (Fig. 3). The mean particle diameter was $14.7 \pm 6.4$ nm ($N = 318$) on the P-face and $15.4 \pm 5.6$ nm ($N = 288$) on the E-face.

Fractures that extended across cortical granules produced images showing at least 2 types of these organelles. In one type of cortical granule (CG I), the contents within the limiting membrane consisted of a central core of tightly-packed particles (about 6–12 nm in diameter) surrounded by a peripheral zone of less compact, circular aggregates measuring 25–50 nm in diameter (Fig. 4d, e). At higher magnification (Fig. 4e), each circular aggregate appeared to be uniformly constructed of 4–6 particles arranged around a central area devoid of particulates. The cortical granules illustrated in the TEM micrograph of Fig. 1b are of this type. In ultrathin sections of well-preserved cortical granules, the circular aggregates appeared as electron-dense bodies joined in linear arrays to form fibrillo-granular meshworks enclosing the core material (Fig. 4f). This array of fiber-like material was occasionally preserved around cores of granules prepared for SEM (Fig. 1a). The contents of the second type of cortical granule (CG II) lacked a compact core with adjacent fibrillar material, and consisted only of small particles enclosed by the perigranular membrane (Fig. 4g).

*The cortical endoplasmic reticulum (CER)*

An elaborate network of smooth cisternae formed the CER. The CER in sections and replicas was typically revealed as a series of isolated circular vesicles and tubular profiles throughout the cortical cytoplasm. Fortuitous fractures through the cortex frequently showed branching CER profiles, thereby affirming the anastomosing nature of the CER membrane complex (Fig. 5a). P- and E-faces of fractured CER elements displayed IMPs of similar density. Regions of close apposition were readily visualized between the CER and the plasma membrane (Fig. 5b) as well as between the CER and

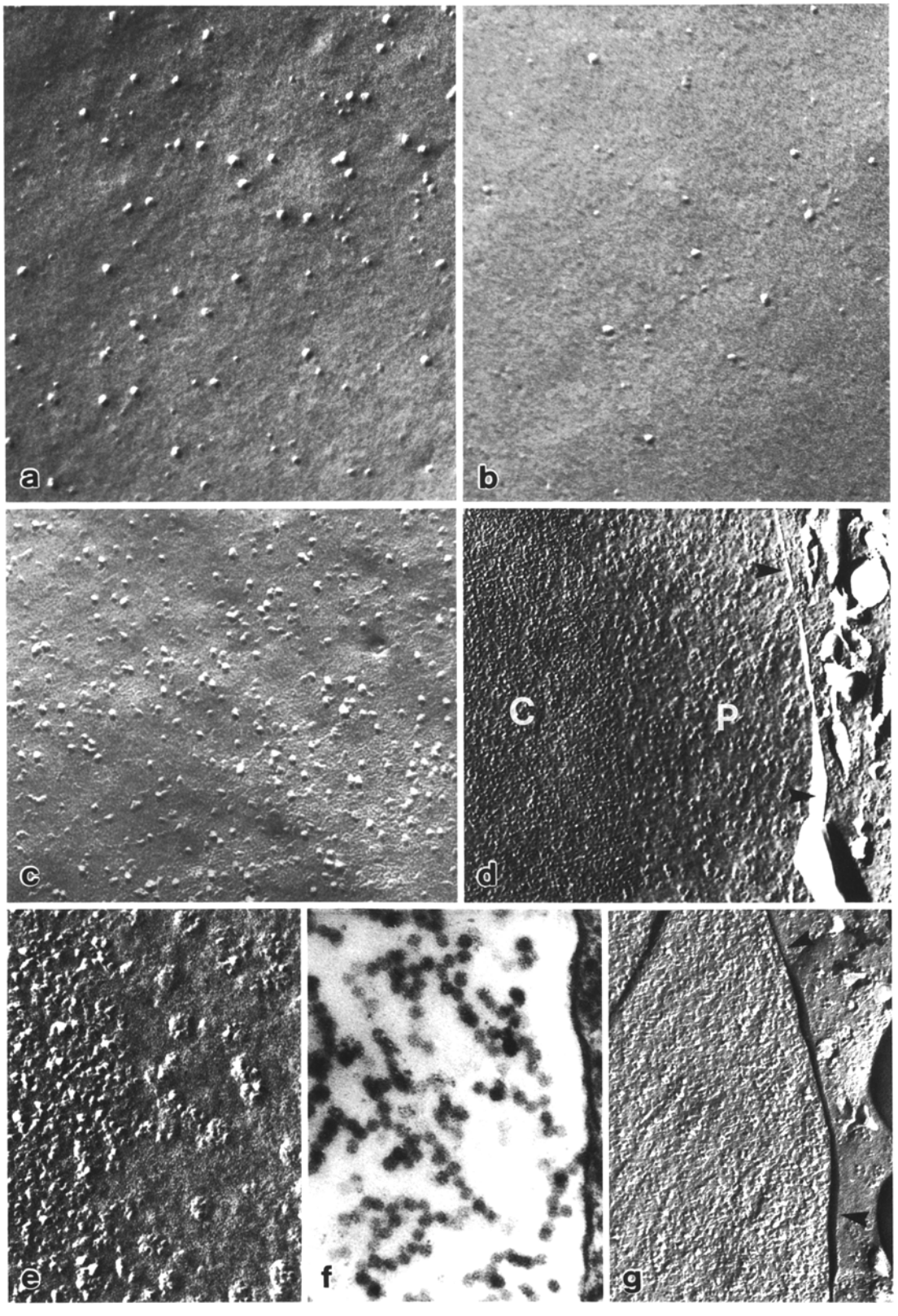


**Fig. 4a–c.** Cortical granules of unactivated egg. **a**, **b** Representative views of IMP density over P- and E-faces, respectively, of cortical granule membranes. ×130000. **c** Representative distribution of IMPs over P-face of egg plasma membrane for comparison with P- and E-faces of cortical granule membranes. ×130000. **d** Representative area of a frozen, cross-fractured type-I cortical granule (CG I) to show central (*C*) and peripheral (*P*) contents within membrane (*arrowheads*). ×17000. **e** Higher magnification of contents of CG I. ×77000. **f** TEM micrograph of fibrillo-granular meshwork formed by peripheral contents of CG I. ×77000. **g** Representative area of frozen, cross-fractured type-II cortical granule showing only small particles within limiting membrane (*arrowheads*). ×77000

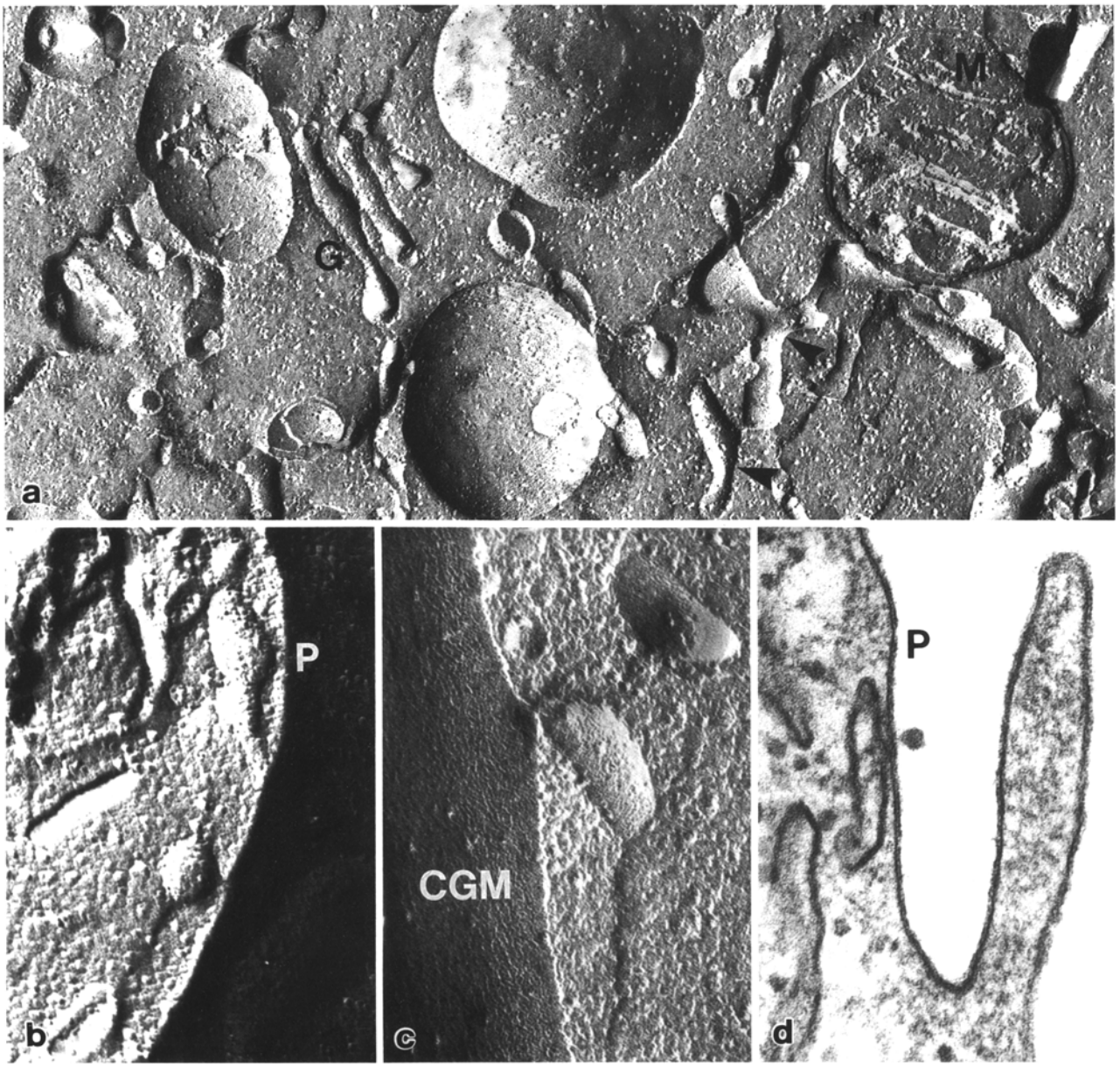


**Fig. 5a–c.** CER of unactivated egg. **a** CER (*arrowheads*) forms elaborate, branching network in cortical cytoplasm. *G* Golgi apparatus; *M* mitochondria. ×50500. **b**, **c** Replicas showing profiles of CER in close apposition with plasma membrane (*P*; ×36000) and cortical granule membrane (*CGM*; ×58000). **d** TEM micrograph showing profile of CER and plasma membrane (*P*) separated by narrow gap. ×123000

membranes of cortical granules (Fig. 5c). In ultrathin sections, membranes of CER profiles were frequently seen to run parallel to the plasma membrane, being separated from it by a narrow gap ranging from 7–10 nm (Fig. 5d). Occasionally, we have detected electron-dense material in the gap.

*The cortex of the activated egg*

Immersion of zebrafish eggs in dechlorinated tank water triggers exocytosis of cortical granules and membrane retrieval (Hart and Yu 1980; Donovan and Hart 1986). Exocytosis is initiated beyond the site of sperm entry by 30 s postactivation; subsequent breakdown of granules occurs randomly over the animal and vegetal poles of the egg for an additional 3–4 min (Hart and Yu 1980; Schalkoff and Hart 1986). In this study, eggs activated for 2–4 min and prepared for either SEM or replication produced expansive views of the reorganized egg surface. SEM images of the egg surface during this time showed a mosaic of two distinguishable membrane domains: the original egg plasma membrane covered with microplicae and the membranes of newly-inserted cortical granules, which were relatively smooth and lacked microplicae (Fig. 6a). Cortical granules undergoing exocytosis varied in their morphology and were identified as either deep

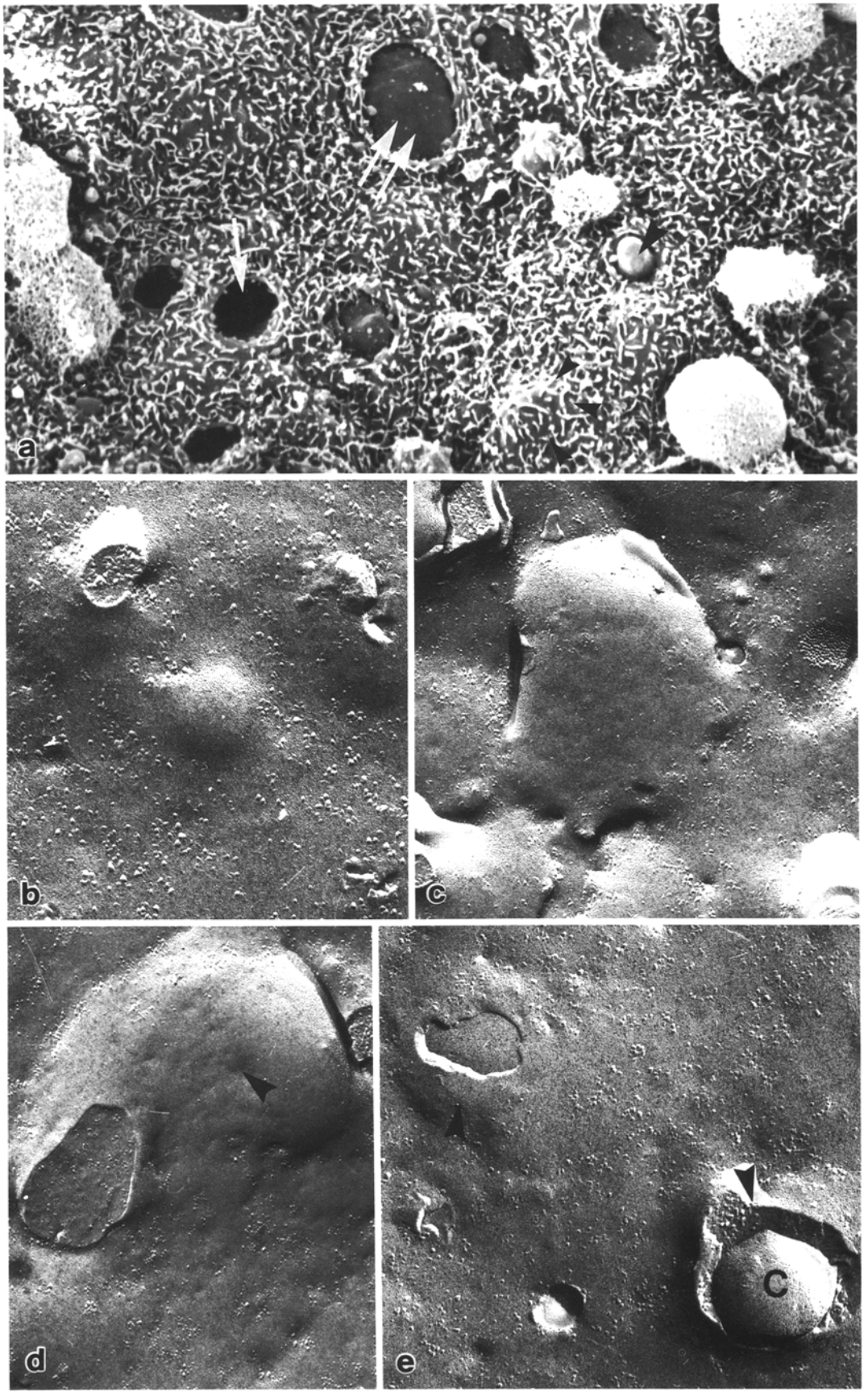


**Fig. 6a–c.** Mosaic plasma membrane and early stages of exocytosis (2 min egg). **a** SEM image showing that cortical granules push-up to form dome-like swelling (*small arrowheads*), rupture, and release contents (*large arrowhead*). Evacuated cortical granules appear as deep crypts (*single arrow*) that become transformed into flattened membrane patches (*double arrows*). ×2400. **b**, **c** P-face replicas of elevated cortical granules showing apparent clearance of IMPs from surface. ×84800. **d** Inward dimple (*arrowhead*) in P-face replica of elevated cortical granule appears to mark site of fusion between plasma and cortical granule membrane. ×59000. **e** P-face replica showing 2 granules (*arrowheads*) in different stages of rupture. *C* E-face of cortical granule. ×71600

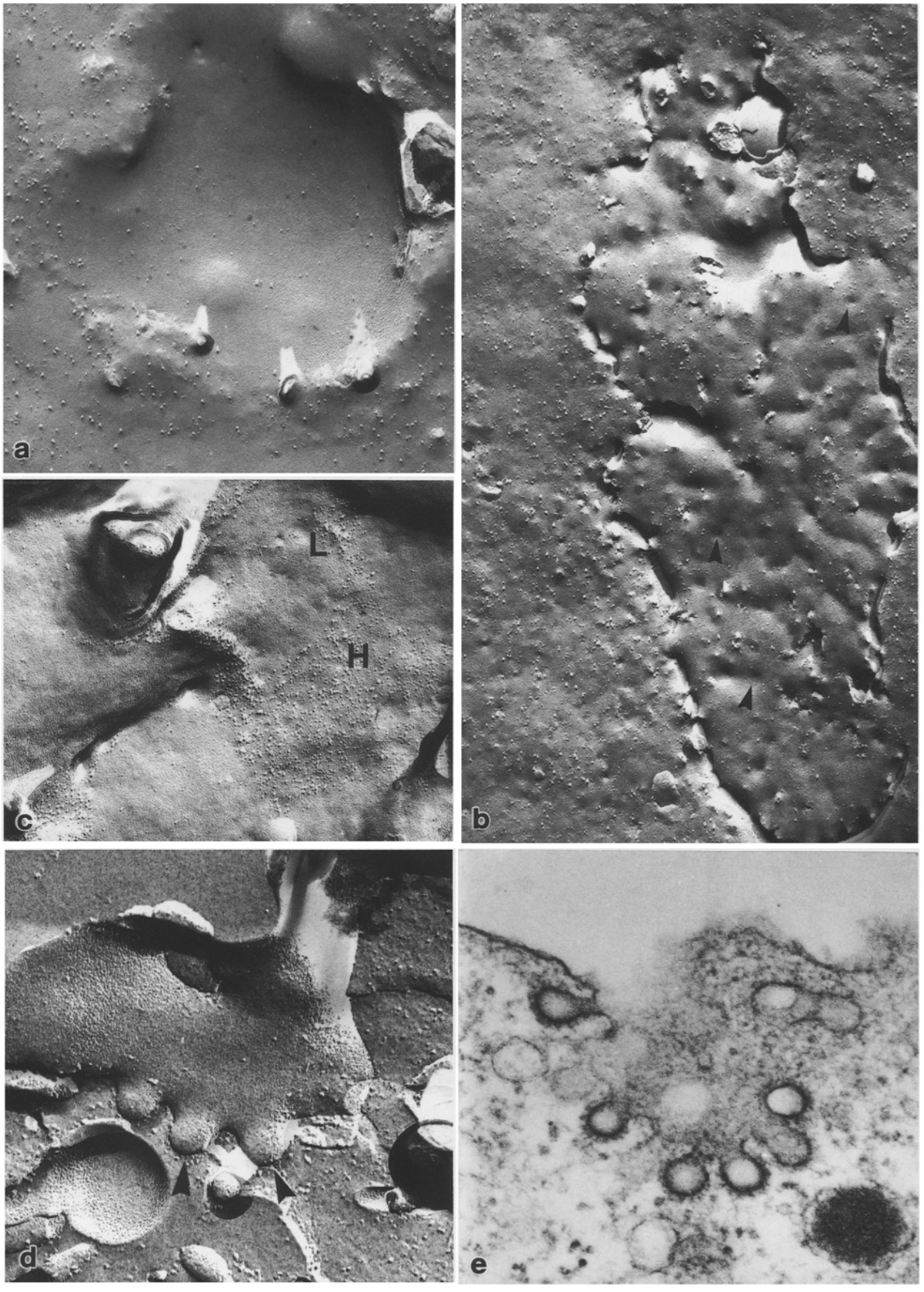


**Fig. 7a–e.** Later stages of cortical granule exocytosis. **a** En face view of evacuated cortical granule showing sharp transition in IMP density between egg plasma membrane and cortical granule membrane. ×41000. **b** Replica of flattened cortical granule membrane patch with possible sites of forming coated vesicles (*arrowheads*). ×46170. **c** P-face replica (4 min egg) of region of plasma membrane free of visible exocytotic profiles and showing areas of high (*H*) and low (*L*) IMP densities. ×49248. **d** En profil view of fractured cortical granule crypt showing attached coated vesicles (*arrowheads*). ×102600. **e** Grazing ultrathin section through cortical granule crypt showing several forming coated vesicles. ×80770

crypts, shallow depressions, or flattened patches of membrane (Fig. 6a).

The exocytosis of individual cortical granules appeared to begin with the organelle pushing-up beneath the egg surface to form a dome-like swelling covered by microplicae (Fig. 6a). Similar deformations of the plasma membrane were visible in P-face fractures prepared from eggs fixed during the cortical reaction (Fig. 6b–d). The top surface of the bulges in the P-face plasma membrane in most, but not all, cases revealed few if any IMPs, indicating a distinct change, with granule elevation, in the distribution of particles in this region (Fig. 6b, c). However, we were unable to detect any change in the distribution of IMPs at the base of such granule swellings. Over a few granules, a small inward dimple was observed within the IMP-free area, suggesting that this might be the initial site of contact or fusion between granule and egg plasma membranes (Fig. 6d). Subsequently, an opening or pore appeared in the elevated granule and resulted in exposure of the granule contents (Fig. 6e).

Recently evacuated cortical granules in P-face fractures of the egg surface were identified as deep pits or crypts with wide openings (Fig. 7a). P-face images of the reorganized surface also revealed concave depressions and flattened patches of membrane confluent with the general contour of the plasma membrane (Fig. 7b). These membrane patches were interpreted as later-stage profiles of cortical granule exocytosis based on our SEM observations and IMP density determinations (Table 1). The shape and size of the flattened patches of membrane were variable. Structural transformation of exocytotic profiles was accompanied by little apparent alteration in the distribution of IMPs. Qualitatively, particle density over the P-face of newly-added cortical granule membrane continued to have the low IMP density that it had before fusion; hence, a distinctive change in IMP density could be seen at the transition between these domains in the mosaic surface (Fig. 7a, b). Quantitative analysis supported this striking difference in IMP density between the two membrane domains (Table 1). The density of particles on the P-face of the cortical granule membrane was higher than that on the same leaflet of intact cortical granules, but this difference was not significant (Table 1). Similarly, the drop in IMP density over the P-face of the plasma membrane of the activated egg was demonstrated not to be significantly different from the same surface of the unactivated egg (Table 1). However, a broader range of IMP sizes and a substantial increase in mean IMP diameter ($23 \pm 7.4$ nm; $N = 119$) were observed over the P-face of the activated egg plasma membrane when compared with the unactivated state (Fig. 3). Differences in IMP density between plasma and cortical granule membrane domains appeared to be maintained even after most profiles of exocytosis had disappeared from the egg surface (Fig. 7c).

We have encountered fractured cortical granule crypts that showed several vesicles, ~90–100 nm in diameter, associated with the limiting membrane (Fig. 7d). These granule profiles displayed a characteristic low IMP density. Grazing sections through cortical granule crypts confirmed the presence of multiple coated vesicles at these sites (Fig. 7e). Rounded depressions were consistently detected over P-face fractures of flattened cortical granule patches (Fig. 7b). These appeared to correspond in size with the forming coated vesicles noted in Fig. 7d, e.

## Discussion

We have used techniques of SEM, TEM, and freeze-fracture to study the zebrafish egg cortex before and during the cortical granule reaction. Prominent features of the unactivated cortex include the cortical granules and a complex, branching CER. As observed in ovulated eggs of *Arbacia* (Luttmer and Longo 1985) and *Xenopus* (Gardiner and Grey 1983; Charbonneau et al. 1986), cisternae of the CER are smooth and form close associations with both the plasma membrane and the limiting membranes of cortical granules. Indeed, the narrow gap reported here between profiles of the CER and the plasma membrane has previously been described as part of a specialized junction between the same membranes in *Xenopus* eggs (Gardiner and Grey 1983). Further study of the structure of this site would be useful because of the proposed role of the CER as a calcium storage site (Jaffe 1983; Poenie and Epel 1987). The release of $Ca^{2+}$ into the cytoplasm is required for exocytosis of cortical granules in fish eggs (Iwamatsu 1989; Iwamatsu et al. 1988).

The cortical granules of the zebrafish egg are membrane-limited, and always separated from the plasma membrane by a layer of specialized dense cytoplasm. This arrangement is similar to other secretory cells (Heuser et al. 1979; Chandler and Heuser 1980), but very different from that of echinoderm eggs in which cortical granules appear to be tethered directly to the plasma membrane (Detering et al. 1977; Longo 1981; Chandler 1984). The narrow, subplasmalemmal layer of cytoplasm between the granules and the oolemma is also present in other teleost eggs (Kobayashi 1985; Ivanenkov et al. 1990) and appears to be enriched with actin filaments (Ivanenkov et al. 1990). Based on studies of somatic cell secretion (Cheek and Burgoyne 1986; Aunis and Bader 1988), it is hypothesized that the subplasmalemmal cytoplasm is a barrier that must be reorganized to allow access of the cortical granules to the oolemma during exocytosis.

Replicas of cross-fractured cortical granules confirm and extend previous observations showing at least 2 types (CG I and II) of these organelles in the cortex (Hart and Yu 1980). Ultrastructurally, CG I is distinguished from CG II by the presence of a compact, particulate core and a distinct peripheral layer of fibrillogranular material beneath the perigranular membrane. The contents of CG II are composed only of particles similar in size to those of the central mass of CG I. We believe that CG I and CG II are equivalent, respectively, to the "dark" and "light" types of cortical granules previously described in this egg (Hart and Yu 1980). Heterogeneity of cortical granules has been reported in other vertebrate

eggs (Campanella and Andreuccetti 1977; Nicosia et al. 1977), but its functional significance is presently unknown. Our results also show that limiting membranes of cortical granules are distinguishable from the plasma membrane by IMP density and size. The P- and E-faces of zebrafish cortical granule membranes exhibit a significantly lower density of IMPs than the P-face of the egg plasma membrane, an observation also reported in echinoderm eggs (Pollock 1978; Longo 1981). The mean IMP diameter on P- and E-faces of cortical granule membranes is virtually identical and substantially larger than that of the P-face of the oolemma.

Collectively, our SEM and freeze-fracture images establish that a predictable sequence of morphological change accompanies the exocytosis of cortical granules. In contrast to echinoderm eggs (Chandler and Heuser 1979), the plasma membrane conforms to the spherical shape of a cortical granule during early stages of exocytosis and forms a distinct dome-shaped elevation or bulge at the surface. Presumably, this configuration represents a state in which the plasma and cortical granule membranes are in close apposition but not yet fused. Clearing of IMPs is frequently observed in the dome-shaped area of the plasma membrane associated with elevated granules. The region cleared of IMPs is generally considered to be an area depleted of membrane proteins, a step required for fusion between the lipid portion of the contacting membranes (Lawson et al. 1977; Orci et al. 1977). However, the question of whether IMPs migrate from sites of exocytosis has been the focus of controversy. Although reported in several secretory cell types (Lawson et al. 1977; Orci et al. 1977; Peixoto de Menezes and Pinto da Silva 1978), particle clearing may be an artifact of either the chemical fixation or glycerination that is used in conventional freeze-fracture (Chandler and Heuser 1979; Chandler 1984). The possibility cannot be excluded that truly IMP-free regions appear in the oolemma prior to fusion with cortical granule membranes, but alternate approaches to preparing zebrafish eggs for freeze-fracture, including rapid freezing, should be undertaken to clarify this issue. The inward depression within the IMP-free area reported here appears to mark sites of membrane fusion and subsequent pore formation as described in amebocytes (Ornberg and Reese 1981).

Evacuated cortical granules undergo striking alterations in shape and become transformed from deep membrane-limited pockets with circular openings to flattened patches of membrane. The change in architecture of the cortical granule profile appears to require the discharge of the granule contents (Chandler et al. 1989). This transformation of an exocytotic profile is reconstructed from fixed images that allow us to identify cortical granule membrane in the mosaic surface during the time-course of granule breakdown. Two features characterize cortical granule membrane profiles. First, both TEM and freeze-fracture clearly show that coated pits and coated vesicles are topographically associated with early profiles of cortical granule exocytosis (Donovan and Hart 1986; this study). Whether membrane retrieval occurs throughout the period of profile reorganization is unclear, although depressions over P-face fractures of flattened cortical granule membranes may also be forming coated vesicles. Presumably, the removal of membrane would alter the morphology of the profile. Second, the low IMP density over crypts and patches of membrane in the mosaic egg surface is reminiscent of the concentration of IMPs over cortical granule membranes of unactivated eggs, and this points to their cortical granule origin.

Analysis of the distribution of IMPs in the P-face of the mosaic egg plasmalemma provides strong evidence that membrane domains derived from the original egg plasma membrane and the cortical granules persist in the recently activated egg, and that the removal of membrane by endocytosis is selective. We detect no significant differences in IMP density between cortical granule membranes of unactivated and activated eggs. Similarly, the higher density of IMPs over the plasma membrane of the unactivated egg is also a consistent feature of the same domain of the activated egg. Hence, based on IMP density, cortical granule and plasma membrane components of the mosaic surface remain identifiable and do not rapidly intermix following exocytosis, as observed in *Arbacia* eggs (Longo 1981). The apparent constraint on lateral diffusion of IMPs between the 2 membrane domains supports other studies showing a reduction in plasma membrane fluidity after fertilization (Johnson and Edidin 1978). The persistence of differences in IMP density between membranes of secretory vesicles and the plasma membrane, as well as the selective retrieval of vesicle membrane following exocytosis, have been reported in other cells (Aunis et al. 1979; Chandler and Heuser 1980; Patzak and Winkler 1986). There is an apparent trend, although not statistically significant, toward fewer but larger IMPs over the egg plasma membrane domain. The basis of the near 3-fold increase in particle-size is unclear from the present study.

The significance of the temporal and morphological coupling of exocytosis/endocytosis in the recently-activated teleost egg remains to be determined. The temporary intercalation of cortical granule membrane into the plasma membrane undoubtedly affects the physiological properties and function of the egg surface. In the medaka egg, for example, potassium permeability elevates during exocytosis, but falls during the period of membrane retrieval (Nuccitelli 1980). If some or all of the IMPs of cortical granules are potassium channels, it is tempting to suggest that the addition and removal of cortical granule membrane could account for the changes in $K^+$ conductance across the activated egg surface. Further studies of the properties of cortical granule membranes should improve understanding of the significance of surface reorganization in the teleost egg.

*Acknowledgements.* This study was supported by a grant from NIH (HD 17467).

## References

Aunis D, Bader MF (1988) The cytoskeleton as a barrier to exocytosis in secretory cells. J Exp Biol 139:253–266

Aunis D, Hesketh JE, Devilliers G (1979) Freeze-fracture study

of the chromaffin cell during exocytosis: evidence for connections between the plasma membrane and secretory granules and for movements of plasma-membrane associated particles. Cell Tissue Res 197:433–441

Branton D, Bullivant S, Gilula NB, Karnovsky MJ, Moor H, Muhlethaler K, Northcote DH, Packer L, Satir B, Satir P, Speth V, Staehlin LA, Steer RL, Weinstein RS (1975) Freeze-etching nomenclature. Science 190:54–56

Campanella C, Andreuccetti P (1977) Ultrastructural observations on cortical endoplasmic reticulum and on residual cortical granules in eggs of *Xenopus laevis*. Dev Biol 56:1–10

Carron C, Longo FJ (1984) Pinocytosis in fertilized sea urchin (*Arbacia punctulata*) eggs. J Exp Zool 231:413–422

Chandler DE (1984) Exocytosis in vitro: ultrastructure of the isolated sea urchin egg cortex as seen in platinum replicas. J Ultrastruct Res 89:198–211

Chandler DE, Heuser JE (1979) Membrane fusion during secretion. Cortical granule exocytosis in sea urchin eggs as studied by quick-freezing and freeze-fracture. J Cell Biol 83:91–108

Chandler DE, Heuser JE (1980) Arrest of membrane fusion: events in mast cells by quick-freezing. J Cell Biol 86:666–674

Chandler DE, Whitaker MW, Zimmerberg J (1989) High molecular weight polymers block cortical granule exocytosis in sea urchin eggs at the level of granule matrix assembly. J Cell Biol 109:1269–1278

Charbonneau M, Grey RD, Baskins RJ, Thomas D (1986) A freeze-fracture study of the cortex of *Xenopus laevis* eggs. Dev Growth Differ 28:75–84

Cheek TR, Burgoyne RD (1986) Nicotine-evoked disassembly of cortical actin filaments in adrenal chromaffin cells. FEBS Lett 207:110–114

Detering NK, Decker GL, Schmell ED, Lennarz WJ (1977) Isolation and characterization of plasma membrane-associated cortical granules from sea urchin eggs. J Cell Biol 75:899–914

Donovan ME, Hart NH (1982) Uptake of ferritin by the mosaic egg surface of *Brachydanio*. J Exp Zool 223:299–304

Donovan ME, Hart NH (1986) Cortical granule exocytosis is coupled with membrane retrieval in eggs of *Brachydanio*. J Exp Zool 237:391–405

Eddy EM, Shapiro BM (1976) Changes in the topography of the sea urchin egg after fertilization. J Cell Biol 71:35–48

Fisher GW, Rebhun LI (1983) Sea urchin egg cortical granule exocytosis is followed by a burst of membrane retrieval via uptake into coated vesicles. Dev Biol 99:456–472

Gardiner DM, Grey RD (1983) Membrane junctions in *Xenopus* eggs: their distribution suggests a role in calcium regulation. J Cell Biol 96:1159–1163

Gilkey JC, Jaffe LF, Ridgway EB, Reynolds GT (1978) A free calcium wave traverses the activating egg of the medaka, *Oryzias latipes*. J Cell Biol 76:448–466

Goodenough UW, Staehlin LA (1971) Structural differentiation of stacked and unstacked chloroplast membranes. J Cell Biol 48:594–619

Hart NH, Messina M (1972) Artificial insemination of ripe eggs in the zebra fish, *Brachydanio rerio*. Copeia 2:302–305

Hart NH, Yu SF (1980) Cortical granule exocytosis and cell surface reorganization in eggs of *Brachydanio*. J Exp Zool 211:137–159

Hart NH, Yu SF, Greenhut VA (1977) Observations on the cortical reaction in eggs of *Brachydanio rerio* as seen with the scanning electron microscope. J Exp Zool 201:325–331

Heuser JE, Reese TS, Dennis MJ, Jan Y, Jan L, Evans L (1979) Synaptic vesicle exocytosis captured by quick freezing correlated with quantal transmitter release. J Cell Biol 81:275–300

Ivanenkov VV, Minin AA, Ozerova SG (1990) Phalloidin inhibits cortical granule exocytosis and ooplasmic segregation in loach eggs. Cell Differ Dev 29:21–36

Iwamatsu T (1989) Exocytosis of cortical alveoli and its initiation time in medaka eggs induced by microinjection of various agents. Dev Growth Differ 31:39–44

Iwamatsu T, Yoshimoto Y, Hiramoto Y (1988) Cytoplasmic $Ca^{2+}$ release induced by microinjection of $Ca^{2+}$ and effects of microinjected divalent cations on $Ca^{2+}$ sequestration and exocytosis of cortical alveoli in the medaka egg. Dev Biol 125:451–457

Jaffe LF (1983) Sources of calcium in egg activation: a review and hypothesis. Dev Biol 99:265–276

Johnson M, Edidin M (1978) Lateral diffusion in plasma membrane of mouse egg is restricted after fertilization. Nature 272:448–450

Kay ES, Shapiro BM (1985) The formation of the fertilization membrane in the sea urchin egg. In: Metz CD, Monroy A (eds) Biology of fertilization. Academic Press, Orlando, pp 45–80

Kobayashi W (1985) Electron microscopic observation of the breakdown of cortical vesicles in the chum salmon egg. J Fac Sci Hokkaido Univ 24:87–102

Lawson D, Raff MC, Gomperts B, Fewtrell C, Gilula NB (1977) Molecular events during membrane fusion: a study of exocytosis in rat peritoneal mast cells. J Cell Biol 72:242–259

Longo FJ (1981) Morphological features of the surface of the sea urchin (*Arbacia punctulata*) egg: oolemma-cortical granule association. Dev Biol 84:173–182

Longo FJ (1988) Reorganization of the egg surface at fertilization. Int Rev Cytol 113:233–269

Luttmer S, Longo FJ (1985) Ultrastructural and morphometric observations of cortical endoplasmic reticulum in *Arbacia*, *Spisula*, and mouse eggs. Dev Growth Differ 27:349–359

Nicosia SJ, Wolf DP, Inoue M (1977) Cortical granule distribution and cell surface characteristics in mouse eggs. Dev Biol 57:56–74

Nuccitelli R (1980) The electrical changes accompanying fertilization and cortical vesicle secretion in the medaka egg. Dev Biol 76:483–498

Orci L, Perrelet A, Friend DS (1977) Freeze-fracture of membrane fusions during exocytosis in pancreatic B-cells. J Cell Biol 75:23–30

Ornberg RL, Reese TS (1981) Beginning of exocytosis captured by rapid-freezing of *Limulus* amebocytes. J Cell Biol 90:40–54

Patzak A, Winkler H (1986) Exocytotic exposure and recycling of membrane antigens of chromaffin granules: ultrastructural evaluation after immunolabeling. J Cell Biol 102:510–515

Peixoto de Menezes A, Pinto da Silva P (1978) Freeze-fracture observations of the lactating rat mammary gland. J Cell Biol 76:767–778

Poenie M, Epel D (1987) Ultrastructural localization of intracellular calcium stores by a new cytochemical method. J Histochem Cytochem 35:939–956

Pollock EG (1978) Fine structural analysis of animal cell surfaces: membranes and cell surface topography. Am Zool 18:25–69

Schalkoff ME, Hart NH (1986) Effects of A23187 upon cortical granule exocytosis in eggs of *Brachydanio*. Roux's Arch Dev Biol 195:35–48

Vater CA, Jackson RC (1989) Purification and characterization of a cortical secretory vesicle membrane fraction. Dev Biol 135:111–123

Yoshimoto Y, Iwamatsu T, Hirano K, Hiramoto Y (1986) The wave pattern of free calcium release upon fertilization in medaka and sand dollar eggs. Dev Growth Differ 28:583–596

Zimmerberg J, Sardet C, Epel D (1985) Exocytosis of sea urchin egg cortical vesicles in vitro is retarded by hyperosmotic sucrose: kinetics of fusion monitored by quantitative light-scattering microscopy. J Cell Biol 101:2398–2410